

Cite this article as: Jiang Longfei, Gong Tianle, Li Pengze, et al. Electrode Potential Explaining the Growth of Anodic Oxides[J]. Rare Metal Materials and Engineering, 2024, 53(09): 2485-2492. DOI: 10.12442/j.issn.1002-185X.20230843.

ARTICLE

# Electrode Potential Explaining the Growth of Anodic Oxides

Jiang Longfei<sup>1</sup>, Gong Tianle<sup>1</sup>, Li Pengze<sup>1</sup>, Zhang Shaoyu<sup>2</sup>, Chen Binye<sup>2</sup>, Zhu Yunxuan<sup>1</sup>, Wang Bing<sup>1</sup>, Zhu Xufei<sup>1</sup>

<sup>1</sup> Key Laboratory of Soft Chemistry and Functional Materials of Ministry of Education, Nanjing University of Science and Technology, Nanjing 210094, China; <sup>2</sup> Jiangsu Urban and Rural Construction College, Changzhou 213147, China

**Abstract:** The formation mechanism of porous anodic oxides remains unclear till now. The classical field-assisted dissolution (FAD) theory cannot explain the relationship between the current curve and FAD reaction, and the influence of the electrode potential on anodization is rarely reported. The electrode potential theory, oxygen bubble model and the ionic current and electronic current theories were introduced to explain the growth of porous anodic oxides of three metals (Ti, Zr and Fe). Taking the anodization of Ti in aqueous solution containing 0.5wt% NH<sub>4</sub>F as an example, the electrode potential was calculated, and the morphology of porous anodic oxides was investigated at low voltages. Results show that the growth of porous anodic oxides is determined by the ratio of the ionic current to the electronic current. During the anodization, metals are classified into two groups: one is easy to form the compact oxide layer, and the other is easy to induce oxygen releasing, thus forming oxygen bubbles. The electrolyte is also classified into two groups correspondingly: compact oxide layer-assisted electrolyte and releasing oxygen-assisted electrolyte.

**Key words:** anodization; electrode potential theory; oxygen bubble model; electronic current; low voltage

Porous anodic oxides obtained by electrochemical anodization or micro-arc oxidation have received much attention as a result of their widespread applications in capacitors, solar panels, etc<sup>[1-7]</sup>. Recently, there are a lot of studies about the growth of porous anodic oxides and the formation mechanism of these porous nanoscale structures remains unclear till now<sup>[8-10]</sup>. Some research data<sup>[11-13]</sup> indicate that anodic TiO<sub>2</sub> nanotubes are a result of the field-assisted dissolution (FAD) of fluoride ions in the electrolyte, but this FAD theory is hard to explain most morphologies of anodic TiO<sub>2</sub> nanotubes and the changing of current-time curves<sup>[14-17]</sup>. For example, it is not able to explain the upward trend of current density-time curves as well as the hemispherical bottom of each anodic TiO<sub>2</sub> nanotube<sup>[16]</sup>. Some researchers built up an oxygen bubble model to explain the complex growth of anodic oxide nanotubes, combined with the ionic current and the electronic current theories<sup>[17-19]</sup>.

However, few of them have proved the growth of nanotubes with quantitative experimental data concerning physical chemistry<sup>[20]</sup>. In this study, the growth of anodic nanotubes was

studied at low voltage and the electrode potential was used to explain the complex morphology of anodic nanotubes. The anodization of Ti leads to the growth of anodic TiO<sub>2</sub> nanotubes at a relatively high voltage<sup>[21-23]</sup>, while at a relatively low voltage, only the compact oxide layer can form. This interesting result can be proved by the oxygen bubble model, ionic current and electronic current theories and the present electrode potential theory. The electrode potential theory suggests different releasing sequences of oxides and oxygen bubbles by quantitatively comparing the electrode potentials of oxygen bubbles and oxides, which has a fundamental influence whether nanotubes or the compact oxide layer can form.

Plus, in a bid to validate the universality of the electrode potential theory, three types of metal were studied: Ti, Zr and Fe. All of them were anodized under low voltage to study the influence of electrode potential on the morphology of anodic nanoscale structures. By comparing morphology of anodic oxide structures, it is found that the electrolyte plays a key role in the growth of anodic oxide structures and that different metals show their specific nature in the anodization. Thus, Ti

Received date: December 27, 2023

Foundation item: National Natural Science Foundation of China (51577093, 51777097); Natural Science Foundation of Jiangsu Higher Education Institutions (20KJB430040); Changzhou Science & Technology Program (CJ20200026); Qing Lan Project in Colleges and Universities of Jiangsu Province

Corresponding author: Zhu Xufei, Ph. D., Professor, Key Laboratory of Soft Chemistry and Functional Materials of Ministry of Education, Nanjing University of Science and Technology, Nanjing 210094, P. R. China, E-mail: xfzhu@njjust.edu.cn

Copyright © 2024, Northwest Institute for Nonferrous Metal Research. Published by Science Press. All rights reserved.

anodized in aqueous solution containing 0.5wt%  $\text{NH}_4\text{F}$  was defined as the standard condition. By comparing the related nature, metals were divided into two groups: one can easily form the compact oxide layer, and the other can release oxygen easily and thus form oxygen bubbles. Electrolytes were also divided into two groups: compact oxide layer-assisted electrolyte and releasing oxygen-assisted electrolyte. Based on the electrode potential theory, this study categorizes metals and electrolytes and is expected to give a deeper and clearer understanding on the growth of anodic oxides.

## 1 Experiment

The experiment is divided into three parts. The details are presented as follows.

### 1.1 Low voltage anodization of Ti and Zr

The titanium foils (purity 99.5%) with 100  $\mu\text{m}$  in thickness were cut into 1.0 cm $\times$ 6.0 cm pieces. To remove the oxide film of the titanium foils, before the anodization, samples were polished by a mixed solution of HF,  $\text{HNO}_3$  and deionized water (1:1:2, volume ratio) for 30 s. Afterward, the samples were put into deionized water for 1 h and then put in air for drying. In anodization, the titanium foil worked as the anode and a graphite plate worked as the cathode. The area of anodization was 1.0 cm $\times$ 2.0 cm on both sides. Anodization was performed in three different solutions: (1) aqueous solution containing 0.5wt%  $\text{NH}_4\text{F}$ ; (2) ethylene glycol solution containing 0.5wt%  $\text{NH}_4\text{F}$  and 2wt%  $\text{H}_2\text{O}$ ; (3) aqueous solution containing 0.5wt%  $\text{NaNO}_3$ . The anodizing voltage was kept at 1, 5 and 9 V. The anodizing time was at 400 s.

The thickness, purity, pretreatment process and anodizing process of zirconium foils were exactly the same as those of titanium foils described above.

### 1.2 Low voltage anodization of Fe

The iron foils with 100  $\mu\text{m}$  in thickness (purity 99.5%) were cut into 1.0 cm $\times$ 6.0 cm pieces. Before the anodization, iron sheets were dipped into aqueous solution containing 6wt%  $\text{H}_3\text{PO}_4$  at 40  $^\circ\text{C}$  for 30 min for polishing. The post-treatment process and anodizing process of the iron foils were exactly the same as those for the titanium foils described in Section 1.1.

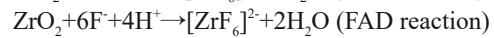
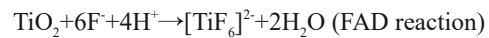
### 1.3 Extra details

The anodizing temperature was kept at 25  $^\circ\text{C}$  via constant temperature water bath. The anodizing current-time curves were recorded by a computer system. After anodization, all the samples (Ti, Zr and Fe) were firstly put into plenty of deionized water for 1 h to clean the remaining electrolyte. Then, they were rinsed by deionized water and dried in air as samples for microstructure observation. Finally, the samples were bent to form the cracks for better view of the cross-sections of the oxide film on the substrate. All the samples were characterized by field emission scanning electron microscope (FESEM, Zeiss Supra 55).

## 2 Results and Discussion

Take the anodization of Ti as an example. According to the

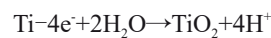
FAD theory<sup>[13,24-26]</sup>, the following reaction firstly occurs during the anodization of Ti:  $\text{Ti}+2\text{H}_2\text{O}\rightarrow\text{TiO}_2+4\text{H}^++4\text{e}^-$ . Then, the fluoride ions in the electrolyte react with  $\text{TiO}_2$  or  $\text{ZrO}_2$ , as follows:



Based on the FAD theory, fluoride ions dissolve the oxide layer from top to bottom, eventually forming porous anodic oxides<sup>[24-26]</sup>. Thompson et al<sup>[27]</sup> pointed out that the above FAD reactions do not contribute to the anodizing current. According to previous findings, nanotube embryos can be seen under the unbroken compact oxide layer, which is opposite to the FAD theory<sup>[28]</sup>. However, the closed gourd-shaped nanotube embryos show that oxygen bubbles play an important role during the growth of nanotubes<sup>[28-31]</sup>. The electrode potential theory is based on the oxygen bubble model as well as the ionic current and the electronic current theory to explain the growth mechanism of nanotubes<sup>[31-33]</sup>.

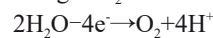
### 2.1 Definition of electrode potential theory

The electrode potential theory thinks that the formation of anodic nanotubes is a result of competition between oxygen bubbles releasing and oxide growth at the anode. Taking the anodization of Ti in aqueous solution containing 0.5wt%  $\text{NH}_4\text{F}$  for example (25  $^\circ\text{C}$ , 101.325 kPa), two reactions occur on the anode:



$$\varphi_{\text{TiO}_2/\text{Ti}}^\theta=-1.06 \text{ V} \quad (1)$$

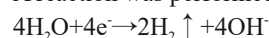
where  $\varphi$  represents the electrode potential in different reactions;  $\varphi_{\text{TiO}_2/\text{Ti}}^\theta$  indicates the standard electrode potential of forming  $\text{TiO}_2$  from Ti.



$$\varphi_{\text{O}_2/\text{H}_2\text{O}}^\theta=1.23 \text{ V} \quad (2)$$

where  $\varphi_{\text{O}_2/\text{H}_2\text{O}}^\theta$  indicates the standard electrode potential of forming  $\text{O}_2$  from  $\text{H}_2\text{O}$ .

A reaction was performed on the cathode.



$$\varphi_{\text{H}_2/\text{H}_2\text{O}}^\theta=-0.83 \text{ V} \quad (3)$$

where  $\varphi_{\text{H}_2/\text{H}_2\text{O}}^\theta$  indicates the standard electrode potential of forming  $\text{H}_2$  from  $\text{H}_2\text{O}$ .

The standard electrode potential of the above reactions is derived from Lange's Handbook of Chemistry<sup>[34]</sup>.

There are two types of total reaction equations in anodizing process:



The above reaction equations are completely consistent with the oxygen bubble model, which can be explained by the electrode potential. The electrode potential theory thinks that the voltage range can be divided into three parts, as shown in Fig.1.

(1) The applied voltage on the samples ( $U$ ) is lower than the decomposition voltage of  $\text{TiO}_2$  ( $U < E_{\text{TiO}_2} \approx -1 \text{ V}$ ). In this range, nothing will be formed because the voltage is lower than the decomposition voltage of both oxides and oxygen bubbles.

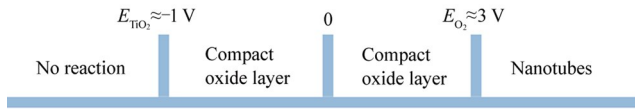


Fig.1 Decomposition voltage in aqueous solution containing 0.5wt% NH<sub>4</sub>F (25 °C and 101.325 kPa) and corresponding compact oxide layer and nanotubes in different voltage sections

(2) The voltage is between the decomposition voltage of TiO<sub>2</sub> and the decomposition voltage of O<sub>2</sub> ( $E_{TiO_2} \approx -1 V < U < E_{O_2} \approx 3 V$ ). In this range, during the anodization, only the compact oxide layer will be formed because the voltage has not reached the decomposition voltage of O<sub>2</sub>, as a result of which, only oxides will grow and form the compact oxide layer.

(3) The voltage is higher than the decomposition voltage of both TiO<sub>2</sub> and O<sub>2</sub> ( $U > E_{O_2} \approx 3 V$ ). In this range, during the anodization, growth of both oxides and oxygen bubbles will occur, which is the basis of the formation of anodic TiO<sub>2</sub> nanotubes. Then, whether anodic TiO<sub>2</sub> nanotubes can be formed is determined by the ratio of the ionic current which forms oxides to the electronic current which forms oxygen bubbles<sup>[30-31]</sup>. The generation of electronic current in micro-arc oxidation coatings is known as the discharge process of sparking or breakdown<sup>[14,35-36]</sup>. According to the ionic current and the electronic current theory<sup>[31-32]</sup>, it can be expressed simply as follows:

$$J_{total} = J_c + J_{ion} \quad (6)$$

$$J_{ion} = A \exp(\beta E) = A \exp(\beta U/d) \quad (7)$$

$$J_c = J_0 \exp(ad) \quad (8)$$

where  $J_{ion}$  is the ionic current which causes the growth of oxides;  $J_c$  is the electronic current which causes the growth of oxygen bubbles to form the anodic TiO<sub>2</sub> nanotubes;  $J_0$  is the initial electronic current<sup>[32]</sup>;  $\alpha$ ,  $\beta$  and  $A$  are the specific proportionality factors that vary significantly with temperatures and electrolytes;  $E$  is the electric field strength;  $d$  is the thickness of the barrier oxide layer<sup>[31]</sup>. The electronic current is in proportional exponential relation with the thickness of the barrier oxide layer  $d$ , while the ionic current shows opposite relationship. When the current shows a downward trend, the ionic current plays a main role in the anodization. When the current shows an upward trend, the electronic current plays a leading role. Only when these two kinds of currents are in the right proportion, anodic TiO<sub>2</sub> nanotubes can be formed, which has been proved under a low temperature.

### 2.2 Explanation of low voltage anodization of Ti by electrode potential theory

Fig.2 shows the FESEM images of Ti anodized at different voltages in aqueous solution containing 0.5wt% NH<sub>4</sub>F for 400 s and the corresponding current density-time curves. It is clear that at 1 V, only the compact oxide layer is formed in Fig.2a. The surface of the compact oxide layer has almost no pits. Fig. 2d also shows that at 1 V, the current drops at the beginning of the anodization and keeps about 0 until the end, which gives a reason why only the compact oxide layer is formed at 1 V. This result is consistent with the electrode potential theory. According to the above theory, when the voltage is between the critical voltage for the generation of titanium oxide and oxygen, only compact oxide layer is generated. Fig.2b shows the morphology of the compact oxide layer anodized at 5 V. There are many pits on the surface of the compact oxide layer. According to the electrode potential

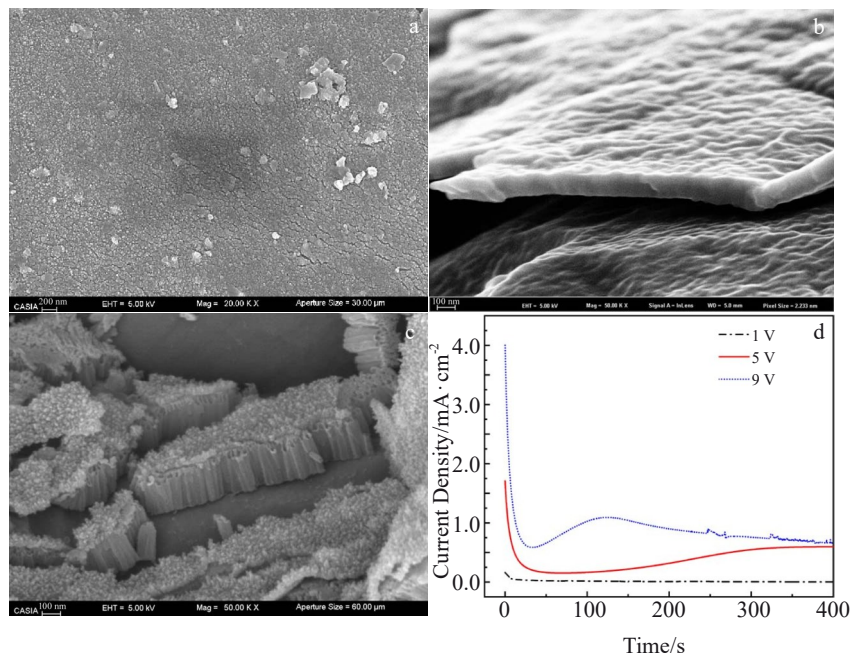


Fig.2 FESEM images of compact oxide layer and anodic TiO<sub>2</sub> nanotubes anodized at 1 V (a), 5 V (b) and 9 V (c) in aqueous solution containing 0.5wt% NH<sub>4</sub>F; corresponding current density-time curves (d)

theory, when the voltage is larger than the decomposition voltage of both  $O_2$  and  $TiO_2$ , two reactions take place on the anode, with the formation of oxides and oxygen bubbles. Fig. 2d shows that after 100 s, the current density-time curve shows an upward trend at 5 V, which indicates that oxygen bubbles exist. Due to the low voltage and short anodizing time, only small craters appear in Fig. 2b and no visible titanium oxide nanotubes form. Fig. 2c illustrates the titanium oxide nanotubes formed at a voltage of 9 V. The corresponding current density-time curve shows that the current density at 9 V is larger than that at 5 V, thus forming the anodic  $TiO_2$  nanotubes. According to the electrode potential theory, when the voltage is larger than the decomposition voltage of both  $O_2$  and  $TiO_2$ , whether anodic  $TiO_2$  nanotubes can be formed is determined by the ratio of the ionic current which causes oxides to the electronic current which causes oxygen bubbles<sup>[17]</sup>. In the current-time curve at 9 V, the decreasing portion of the curve indicates the ionic current and the increasing portion indicates the electronic current. The lowest point of Fig. 2d corresponds to the ionic current, which is about  $0.6 \text{ mA/cm}^2$ . The current that rises from the lowest point ( $0.6 \text{ mA/cm}^2$ ) to the highest point ( $1.1 \text{ mA/cm}^2$ ) is the electronic current (about  $0.5 \text{ mA/cm}^2$ ), and the time to reach the highest point is about 106 s. After the highest point, the ionic current is maintained at  $0.6 \text{ mA/cm}^2$ , and the electronic current decreases gradually, which results in a gradual decrease in the total current.

In this research, anodic oxidation of titanium in electrolyte with 0.5wt%  $NH_4F$  ( $25^\circ \text{C}$ , 101.325 kPa) was used as the standard experimental condition. The following metals and electrolytes are divided into two groups: compact oxide layer

metal (easy to form the compact oxide layer) and releasing oxygen metal (easy to form oxygen bubbles). Electrolytes are divided into two groups: compact oxide layer-assisted electrolyte and releasing oxygen-assisted electrolyte.

Fig. 3 shows the FESEM images of Ti anodized in ethylene glycol solution containing 0.5wt%  $NH_4F+2\text{wt}\% \text{H}_2\text{O}$  and aqueous solution containing 0.5wt%  $NaNO_3$ , and corresponding current density-time curves. Fig. 3a shows that the anodization of Ti cannot form anodic  $TiO_2$  nanotubes at 9 V. The difference between the ethylene glycol solution and the aqueous solution containing 0.5wt%  $NH_4F$  is that the main solvent in electrolyte is ethylene glycol, which is a kind of organic solvent. Tremendous experiments have shown that the organic solvent is more capable of standing the high voltage<sup>[29-31]</sup>. Fig. 3b shows that at 1 and 5 V, the current density-time curves show a downward trend, which indicates that only the compact oxide layer can form. Although the current density-time curve is similar to that at 9 V in aqueous solution containing 0.5wt%  $NH_4F$  shown in Fig. 1d, only the compact oxide layer is formed in the ethylene glycol solution containing 0.5wt%  $NH_4F+2\text{wt}\% \text{H}_2\text{O}$ . According to the electrode potential theory, the ethylene glycol solution containing 0.5wt%  $NH_4F+2\text{wt}\% \text{H}_2\text{O}$  is compact oxide layer-assisted electrolyte and titanium is used as the substrate of compact oxide layer. In this electrolyte, the compact oxide layer is easier to form. As a result, nanotubes formed in this kind of electrolyte contain more oxides, and the ratio of the length to the diameter is smaller.

Fig. 3c shows that at 9 V, the anodization of Ti in aqueous solution containing 0.5wt%  $NaNO_3$  also cannot form anodic  $TiO_2$  nanotubes. The corresponding current density-time curve

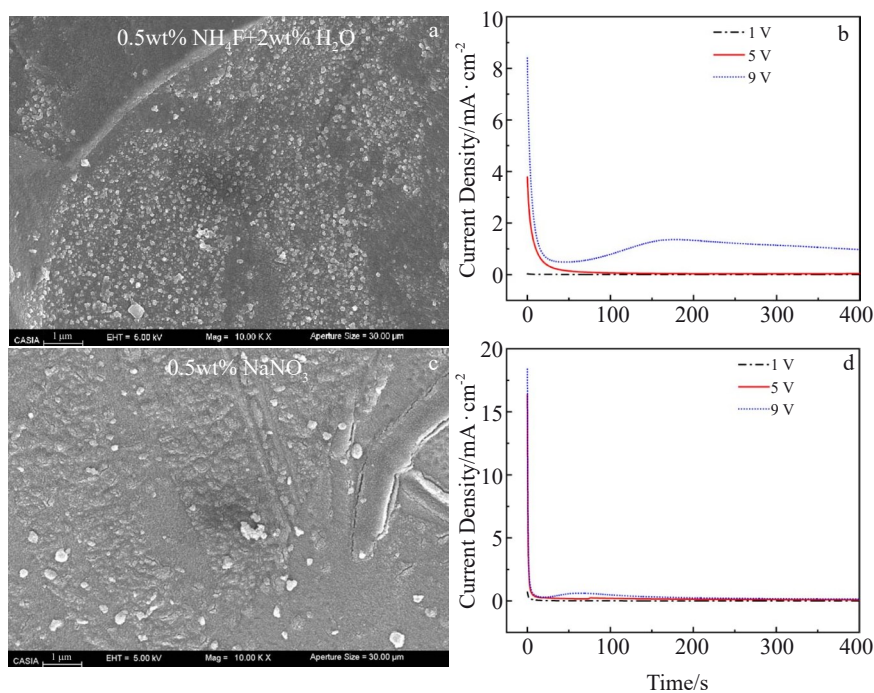


Fig. 3 FESEM images of compact oxide layer of  $TiO_2$  anodized in two different electrolytes at 9 V (a, c) and corresponding current density-time curves (b, d): (a–b) ethylene glycol solution containing 0.5wt%  $NH_4F+2\text{wt}\% \text{H}_2\text{O}$  and (c–d) aqueous solution containing 0.5wt%  $NaNO_3$

in Fig.3d shows almost no upward trend, which indicates that in this kind of electrolyte, the formation of anodic TiO<sub>2</sub> nanotubes is difficult to achieve. With the voltage declining, the current density-time curve shows almost no upward trend, which indicates that the electronic current is too small to release oxygen bubbles and thus the anodic TiO<sub>2</sub> nanotubes hardly form. According to the electrode potential theory, the aqueous solution containing 0.5wt% NaNO<sub>3</sub> is compact oxide layer-assisted electrolyte and Ti is a compact oxide layer metal in this anodization process. Also, the effect of this compact oxide layer-assisted electrolyte is stronger than the ethylene glycol solution containing 0.5wt% NH<sub>4</sub>F+2wt% H<sub>2</sub>O in the anodization of Ti.

### 2.3 Explanation of low voltage anodization of Zr by electrode potential theory

Fig. 4 shows the FESEM images of Zr anodized in three kinds of electrolytes: aqueous solution containing 0.5wt% NH<sub>4</sub>F, ethylene glycol solution containing 0.5wt% NH<sub>4</sub>F+2wt% H<sub>2</sub>O and aqueous solution containing 0.5wt% NaNO<sub>3</sub>, as well as corresponding current density-time curves. Fig.4a shows that at 9 V, the anodization of Zr in aqueous solution containing 0.5wt% NH<sub>4</sub>F can form anodic ZrO<sub>2</sub> nanotubes. The anodic ZrO<sub>2</sub> nanotubes formed in aqueous solution containing 0.5wt% NH<sub>4</sub>F have a larger ratio of length to diameter compared with anodic TiO<sub>2</sub> nanotubes formed in the same electrolyte<sup>[37]</sup>. The FAD theory thinks that it is the upward trend of the current density that forms nanotubes, but in the present condition, there is only the downward trend. It is thought that porous anodic oxides form on one side (the metal/oxide interface) and are dissolved on the other side (the oxide/electrolyte interface)<sup>[13,24]</sup>. However, how it keeps the

same rate of dissolution and growth is not clear, and the FAD reaction has been denied by the flow model of the porous anodic film<sup>[38-39]</sup>. It is impossible to maintain the equilibrium between oxide growth and dissolution<sup>[15-16]</sup>. It is difficult to explain the special morphologies of nanotubes by the FAD theory<sup>[15-17,28]</sup>. Interestingly, the downward trend of the current density-time curve in Fig.4b is relatively small compared to the downward trend in the anodization of Ti in Fig.3b. This can be explained clearly by the ionic current and the electronic current theories. The ionic current takes a leading role when the current shows a downward trend. The smaller the downward trend, the weaker the leading role of ionic current. The ionic current dominates the formation of oxides. As a result, fewer oxides are produced and the nanotubes are thinner, leading to the high ratio of the length to the diameter.

Fig.4b shows that with the voltage declining, the downward trend of current density-time curves becomes weaker. At 1 V, the current density-time curve even shows an upward trend. It indicates that at the beginning of the anodization, the electronic current plays a dominant role, which releases oxygen bubbles. According to the electrode potential theory, aqueous solution containing 0.5wt% NH<sub>4</sub>F is releasing oxygen-assisted electrolyte and Zr is converted to metal oxide in this anodization process of Zr.

Fig.4c shows that at 9 V, the anodization of Zr in ethylene glycol solution containing 0.5wt% NH<sub>4</sub>F+2wt% H<sub>2</sub>O can only form the compact oxide layer with tremendous pits on the surface. Different from the surface with some pits in Fig.3a, the compact oxide layer formed in the anodization of Zr is fluffier, which indicates that lots of oxygen bubbles are released from the surface. Fig.4d shows that the downward

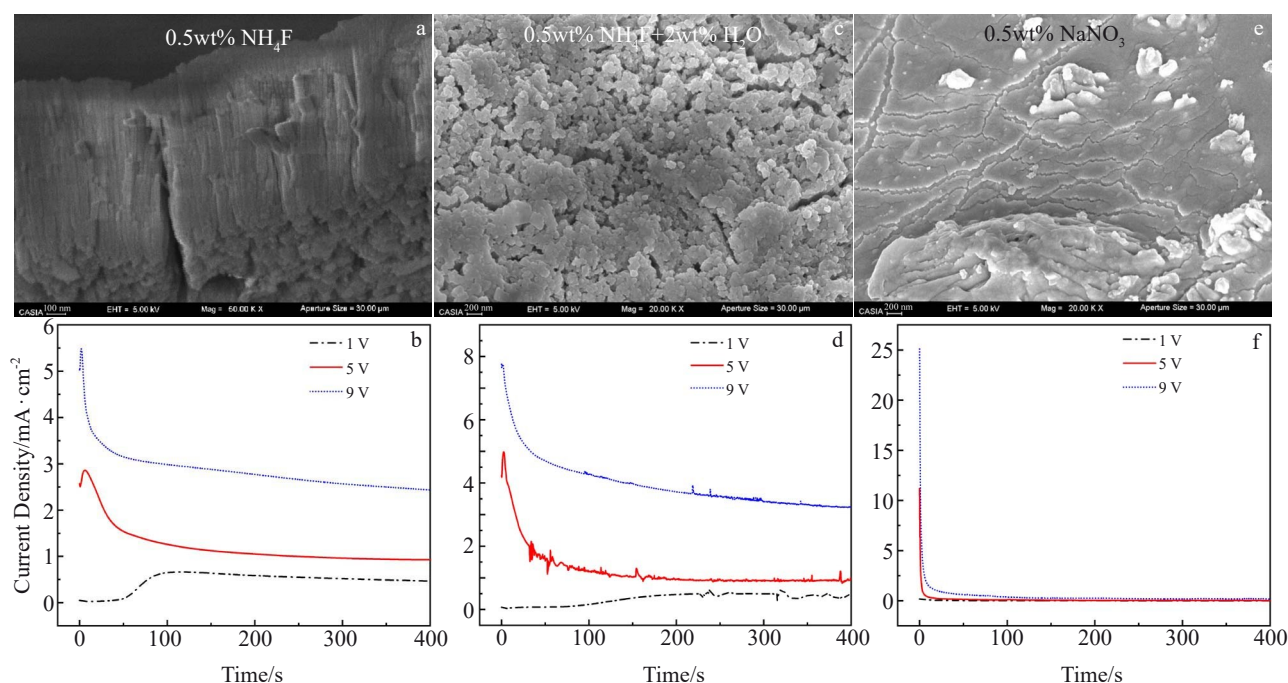


Fig.4 FESEM images of compact oxide layer and the anodic ZrO<sub>2</sub> nanotubes anodized in three kinds of electrolytes at 9 V (a, c, e) and corresponding current density-time curves (b, d, f): (a–b) aqueous solution containing 0.5wt% NH<sub>4</sub>F, (c–d) ethylene glycol solution containing 0.5wt% NH<sub>4</sub>F+2wt% H<sub>2</sub>O, and (e–f) aqueous solution containing 0.5wt% NaNO<sub>3</sub>

trend of the current density-time curve is relatively weaker compared to that in Fig. 3b. With the voltage declining, the downward trend of the current density-time also becomes weaker. According to the electrode potential theory, ethylene glycol solution containing 0.5wt%  $\text{NH}_4\text{F}$ +2wt%  $\text{H}_2\text{O}$  is releasing oxygen-assisted electrolyte and Zr is releasing oxygen metal in this anodization process of Zr.

Fig. 4e shows that at 9 V, the anodization of Zr in aqueous solution containing 0.5wt%  $\text{NaNO}_3$  can only form the compact oxide layer. On the surface, there is almost no pit. Also, similar to Fig. 3d, the current density-time curve shows a sharp downward trend in Fig. 4f, which indicates that during the anodization, only the ionic current exists. According to the electrode potential theory, aqueous solution containing 0.5wt%  $\text{NaNO}_3$  is a compact oxide layer-assisted electrolyte and Zr can generate compact oxide layer in this anodization process of Zr.

#### 2.4 Explanation of low voltage anodization of Fe by electrode potential theory

Fig. 5 shows the FESEM images of Fe anodized in three kinds of electrolytes: aqueous solution containing 0.5wt%  $\text{NH}_4\text{F}$ , ethylene glycol solution containing 0.5wt%  $\text{NH}_4\text{F}$ +2wt%  $\text{H}_2\text{O}$  and aqueous solution containing 0.5wt%  $\text{NaNO}_3$ , as well as corresponding current density-time curves. Fig. 5a shows that at 9 V, the anodization of Fe in aqueous solution containing 0.5wt%  $\text{NH}_4\text{F}$  can form anodic  $\text{Fe}_2\text{O}_3$  nanoflowers. Fig. 5b shows that at 9 V, the current density-time curve shows downward trend at the beginning of the anodization, and the ionic current takes the lead role. Afterwards, the electronic current dominates and releases oxygen bubbles, thus forming the anodic  $\text{Fe}_2\text{O}_3$  nanoflowers. At 5 V, the current density-time

curve also shows a typical trend. However, at 1 V, the current density is almost 0 V, which indicates that 1 V is lower than the decomposition voltage of both the  $\text{Fe}_2\text{O}_3$  and  $\text{O}_2$  in this electrolyte. According to the electrode potential theory, aqueous solution containing 0.5wt%  $\text{NH}_4\text{F}$  is a compact oxide layer-assisted electrolyte and Fe can generate compact metal oxides in this anodization process of Fe.

Fig. 5c shows that at 9 V, the anodization of Fe in ethylene glycol solution containing 0.5wt%  $\text{NH}_4\text{F}$ +2wt%  $\text{H}_2\text{O}$  can only form the compact oxide layer with lots of pits, which is similar to the anodization of Zr in Fig. 4c. These pits on the surface of the compact oxide layer are caused by the electronic current, which releases oxygen bubbles. Fig. 5d shows that with the voltage declining, the downward trend of the current density-time curve is weaker. Also, the current density at 1 V is 0 V, which indicates that 1 V is lower than the decomposition voltage of both the  $\text{Fe}_2\text{O}_3$  and  $\text{O}_2$  in this electrolyte. According to the electrode potential theory, ethylene glycol solution containing 0.5wt%  $\text{NH}_4\text{F}$ +2wt%  $\text{H}_2\text{O}$  is releasing oxygen-assisted electrolyte and Fe is releasing oxygen metal in this anodization process of Fe<sup>[40]</sup>.

Fig. 5e shows that at 9 V, the anodization of Fe in aqueous solution containing 0.5wt%  $\text{NaNO}_3$  can form anodic  $\text{Fe}_2\text{O}_3$  nanoflower embryos. The nanoflower embryos in Fig. 5e grow disorderly. Fig. 5f shows that in aqueous solution containing 0.5wt%  $\text{NaNO}_3$ . With the voltage declining, the current density always shows a sharp downward trend. It indicates that the ionic current takes the leading role and forms oxides. The electronic current is so weak that few oxygen bubbles are released. According to the electrode potential theory, aqueous solution containing 0.5wt%  $\text{NaNO}_3$  is a compact oxide layer-

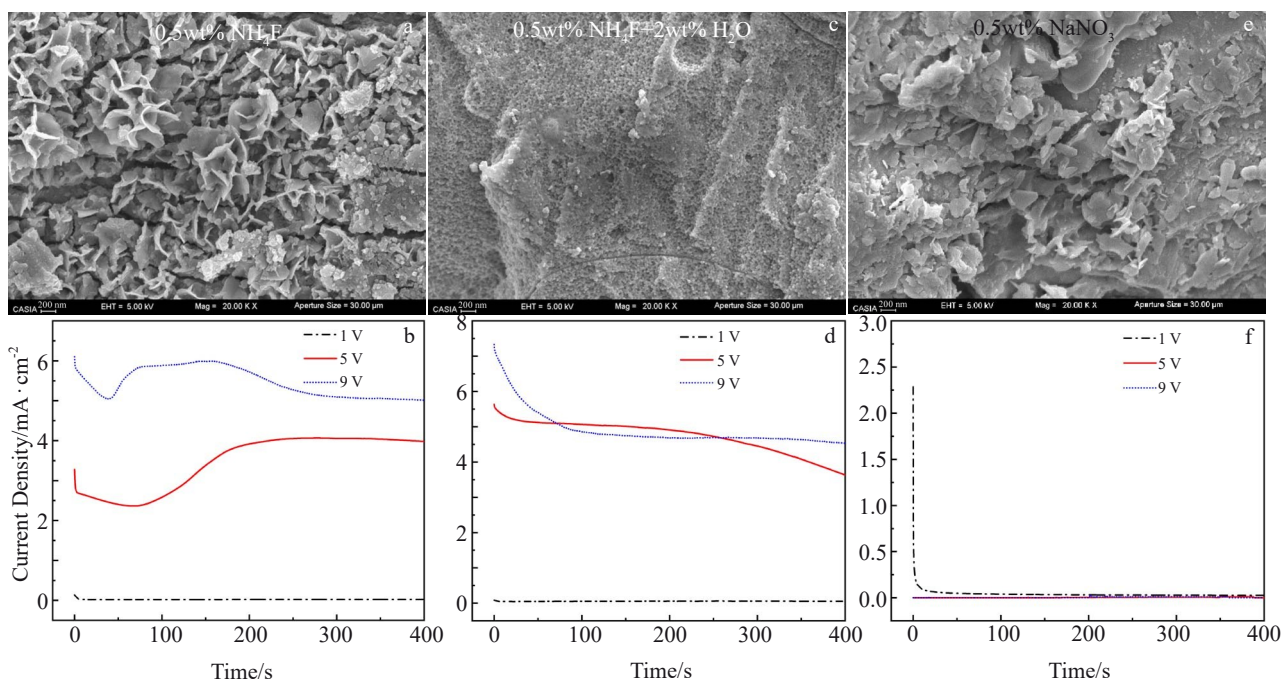


Fig.5 FESEM images of the compact oxide layer and the anodic  $\text{Fe}_2\text{O}_3$  nanoflowers anodized in three kinds of electrolytes at 9 V (a, c, e) and corresponding current density-time curves (b, d, f): (a–b) aqueous solution containing 0.5wt%  $\text{NH}_4\text{F}$ , (c–d) ethylene glycol solution containing 0.5wt%  $\text{NH}_4\text{F}$ +2wt%  $\text{H}_2\text{O}$ , and (e–f) aqueous solution containing 0.5wt%  $\text{NaNO}_3$

**Table 1** Classification of the electrolytes as compact oxide layer-assisted electrolyte or releasing oxygen-assisted electrolyte

Electrolyte	Aqueous solution containing 0.5wt% NH <sub>4</sub> F	Ethylene glycol solution containing 0.5wt% NH <sub>4</sub> F +2wt% H <sub>2</sub> O	Aqueous solution containing 0.5wt% NaNO <sub>3</sub>
Ti	Standard condition	Compact oxide layer-assisted electrolyte	Compact oxide layer-assisted electrolyte
Zr	Releasing oxygen-assisted electrolyte	Releasing oxygen-assisted electrolyte	Compact oxide layer-assisted electrolyte
Fe	Compact oxide layer-assisted electrolyte	Releasing oxygen-assisted electrolyte	Compact oxide layer-assisted electrolyte

assisted electrolyte and Fe can generate compact metal oxides in this anodization process of Fe.

### 2.5 Specific evaluation criteria for the classification of electrolytes and metals by electrode potential theory

Table 1 shows the classification of the electrolyte which is easy to form the compact oxide layer or to release oxygen bubbles. Whether the electrolyte is a compact oxide layer-assisted electrolyte or a releasing oxygen-assisted electrolyte is determined by the change trend of the current density-time curve with the voltage declining. If the downward trend of the current density-time curve is weaker as the voltage declines (like Fig. 4b), it is a kind of releasing oxygen-assisted electrolyte. This is because the downward trend represents the ionic current while the upward trend represents the electronic current<sup>[17]</sup>. With the voltage declining, the downward trend of the current density-time curve is weaker so the electronic current occupies a larger proportion, which indicates that oxygen bubbles are easier to release. The aqueous solution containing 0.5wt% NaNO<sub>3</sub> is a strong compact oxide layer-assisted electrolyte, as the current density-time curve shows a sharp downward trend.

### 3 Conclusions

1) The electrode potential theory thinks that the electrode potential of metal and O<sub>2</sub> on the anode determines the trend of the current density-time curve and the morphology of porous anodic oxides. If the voltage is higher than the decomposition voltage of both metals and O<sub>2</sub>, the current will be distributed in proportion, which can be explained clearly by the ionic current and electronic current theory.

2) It is calculated that the decomposition voltage of TiO<sub>2</sub> is about -1 V and the decomposition of O<sub>2</sub> is about 3 V. When the voltage is 5 V, there are many pits on the surface of the compact oxide layer, which indicates that some oxygen bubbles are released from the surface since the voltage is not high enough. At 9 V, anodic TiO<sub>2</sub> nanotubes are formed, which verifies the correctness of the electrode potential theory and the oxygen bubble model.

3) Electrolytes can be divided into two groups: compact oxide layer-assisted electrolyte and releasing oxygen-assisted electrolyte. The aqueous solution containing 0.5wt% NaNO<sub>3</sub> is a strong compact oxide layer-assisted electrolyte, in which the nanotubes hardly form and only the compact oxide layer can form. Metals are also divided into two groups for their

morphology: compact oxide layer metal and releasing oxygen metal. Ti is more prone to oxide formation compared with Zr, so the ratio of the length to the diameter of ZrO<sub>2</sub> is much larger than that of TiO<sub>2</sub>.

### References

- Lü Kai, Guo Baoquan, Zhang Yaping et al. *Rare Metal Materials and Engineering*[J], 2019, 48(8): 2474
- Guo Yupeng, Di Shichun, Lü Pengxiang et al. *Rare Metal Materials and Engineering*[J], 2015, 44(9): 2240 (in Chinese)
- Ji X, Zhang H T, Ye N C et al. *Molecular Catalysis*[J], 2023, 549: 113463
- Chai Ruxia, He Zhifeng, Xia Yafeng et al. *Titanium Industry Progress*[J], 2024, 41(1): 41 (in Chinese)
- Nan Rong, Cai Jianhua, Yang Jian et al. *Titanium Industry Progress*[J], 2023, 40(5): 40 (in Chinese)
- Wang Q Y, Zhao Y H, Zhang Z F et al. *Ceramics International*[J], 2023, 49(4): 5977
- Xu D Y, Zhao H, Zhen C M. *Microporous and Mesoporous Materials*[J], 2024, 363: 112849
- Zhang W G, Sun Y T, Tian R F et al. *Surface & Coatings Technology*[J], 2023, 469: 129783
- Zhang Y, Chen Y Z, Liu Y et al. *Rare Metal Materials and Engineering*[J], 2024, 53(5): 1310
- Broens M I, Cervantes W R, Collao A M A et al. *Journal of Electroanalytical Chemistry*[J], 2023, 935: 117314
- Leclere D J, Velota A, Skeldon P et al. *Journal of The Electrochemical Society*[J], 2008, 155(9): C487
- Hebert K R, Albu S P, Paramasivam I et al. *Nature Materials*[J], 2012, 11(2): 162
- Kowalski D, Kim D, Schmuki P et al. *Nano Today*[J], 2013, 8(3): 235
- Wang X M, Zhang F Q. *Transactions of Nonferrous Metals Society of China*[J], 2022, 32(7): 2243
- Yu M S, Cui H M, Ai F P et al. *Electrochemistry Communications*[J], 2018, 86: 80
- Zhang Z Y, Liu Q Q, He M F et al. *Journal of The Electrochemical Society*[J], 2020, 167(11): 113501
- Peng K W, Liu L, Zhang J Z et al. *Electrochemistry Communications*[J], 2023, 148: 107457

- 18 Cao J W, Gao Z Q, Wang C et al. *Surface & Coatings Technology*[J], 2020, 388: 125592
- 19 Liao L, Huang W G, Cai F G et al. *Journal of Materials Science-Materials in Electronics*[J], 2021, 32(7): 9540
- 20 Zhou X Y, Ma C Y, Yang J et al. *Rare Metal Materials and Engineering*[J], 2018, 47(10): 3008
- 21 Xiao T T, Zhao J L, Wang X L et al. *Materials Chemistry and Physics*[J], 2020, 240: 122179
- 22 Cao S K, Huang W Q, Wu L Z et al. *Langmuir*[J], 2018, 34(46): 13888
- 23 Bai L, Zhao Y, Chen P R et al. *Small*[J], 2021, 17(4): 2006287
- 24 Zhou X M, Nguyen N T, Özkan S et al. *Electrochemistry Communications*[J], 2014, 46: 157
- 25 Patel S N, Jayaram V, Banerjee D. *Surface & Coatings Technology*[J], 2017, 323: 2
- 26 Ni Y L, Li C Y, Chen J D et al. *Ceramics International*[J], 2022, 48(1): 495
- 27 Oh J, Thompson C V. *Electrochimica Acta*[J], 2011, 56(11): 4044
- 28 Gong T L, Li C Y, Li X et al. *Nanoscale Advances*[J], 2021, 3(16): 4659
- 29 Deng P Y, Bai X D, Chen X W et al. *Journal of The Electrochemical Society*[J], 2004, 151(5): B284
- 30 Zhu X F, Liu L, Song Y et al. *Monatshefte für Chemie*[J], 2008, 139(9): 999
- 31 Zhu X F, Song Y, Liu L et al. *Nanotechnology*[J], 2009, 20(47): 475303
- 32 Albella J M, Montero I, Martinez-Duart J M. *Electrochimica Acta*[J], 1987, 32(2): 255
- 33 Li C Y, Luo K, Yan B W et al. *The Journal of Physical Chemistry C*[J], 2023, 127(20): 9707
- 34 Dean J A. *Mater Manuf Process*[J], 1978, 5(4): 687
- 35 Zhang Y, Li P Z, Wang S Y et al. *The Journal of Physical Chemistry C*[J], 2023, 127(32): 16148
- 36 Zhu X F, Han H, Song Y et al. *Acta Physica Sinica*[J], 2012, 61(22): 228202
- 37 Wang A C, Li C Y, Jiang L F et al. *Ceramics International*[J], 2022, 48(19): 27703
- 38 Garacia-Vergara S J, Skeldon P, Thompson G E et al. *Electrochimica Acta*[J], 2006, 52(2): 681
- 39 Houser J E, Hebert K R. *Nature Materials*[J], 2009, 8(5): 415
- 40 Martin-Gonzalez M, Martinez-Moro R, Aguirre M H et al. *Electrochimica Acta*[J], 2020, 330: 135241

## 电极电位解释阳极氧化物的生长

蒋龙飞<sup>1</sup>, 龚天乐<sup>1</sup>, 李鹏泽<sup>1</sup>, 张少瑜<sup>2</sup>, 陈滨掖<sup>2</sup>, 朱云暄<sup>1</sup>, 王冰<sup>1</sup>, 朱绪飞<sup>1</sup>

(1. 南京理工大学 软化学与功能材料教育部重点实验室, 江苏 南京 210094)

(2. 江苏城乡建设职业学院, 江苏 常州 213147)

**摘要:** 多孔阳极氧化物的形成机理至今仍不清楚。研究者倾向于用物理模型来解释它们的生长机理, 很少报道电极电位对阳极氧化的影响, 因为阳极氧化电压远远高于电极电位。创新性地引入电极电位理论、氧气气泡模型以及离子电流和电子电流理论来解释3种金属(Ti、Zr和Fe)在低电压下多孔阳极氧化物的生长机理。以Ti在0.5% (质量分数)  $\text{NH}_4\text{F}$ 水溶液中的阳极氧化为例, 计算了电极电位, 解释了在低电压下多孔阳极氧化物的形貌。结果表明, 多孔阳极氧化物的生长由离子电流和电子电流的比值决定。阳极氧化过程中的金属分为2类: 一类是容易形成致密氧化层的金属, 另一类是容易导致氧气析出的金属。相应的, 电解液也被分为2类: 容易形成致密氧化层的电解液和容易导致氧气析出的电解液。

**关键词:** 阳极氧化; 电极电势理论; 氧气气泡模型; 电子电流; 低电压

作者简介: 蒋龙飞, 男, 1988年生, 博士生, 南京理工大学软化学与功能材料教育部重点实验室, 江苏 南京 210094, E-mail: jlf@njjust.edu.cn